Predicting the Distribution of Contamination from a Chlorinated Hydrocarbon Release

Mark J. Lupo

K. W. Brown Environmental Services
501 Graham Road, College Station, TX 77845

George J. Moridis

Earth Sciences Division, Lawrence Berkeley Laboratory
University of California, Berkeley, CA 94720

Introduction

The T2VOC model (Falta et al., 1995) with the T2CG1 conjugate gradient package (Moridis and Pruess, 1995) was used to simulate the motion of a dense chlorinated hydrocarbon plume released from an industrial plant. The release involved thousands of kilograms of trichloroethylene (TCE) and other chemicals that were disposed of onsite over a period of nearly twenty years. After the disposal practice ceased, an elongated plume was discovered. Because much of the plume underlies a developed area, it was of interest to study the migration history of the plume to determine the distribution of the contamination.

Procedure

The transport modeling approach in a typical environmental consulting firm would involve the use of a groundwater model to simulate the flow through the saturated zone. A vadose zone model could then be used to study the upward transport of contaminants into overlying buildings. However, the chemicals were poured into a well installed in the vadose zone. There have been field studies to demonstrate that the initial distribution of chlorinated hydrocarbons in the subsurface has a significant bearing on their transport and detectability in a soil-gas survey (Rivett, 1995). A source in the vadose zone, such as the one simulated by T2VOC in this study, and a source beneath the water table will yield very different transport histories and surface fluxes.

The sloped, coarse unsaturated material at the simulated site is underlain by highly fractured bedrock. The chlorinated chemicals released were dense but volatile, indicating that density driven vapor flow could be important. The release was of a great enough magnitude that dense nonaqueous phase liquids (DNAPLs) should be present. Field measurements showed that DNAPL did exist and that TCE was detectable at great depth in the underlying bedrock. This further suggested that the best approach would involve a multicomponent model capable of simulating the vadose zone as well as the saturated zone. In this way, a single code could be used to accurately simulate both the lateral and vertical transport of the TCE.

The plume of interest was several kilometers in length and up to 500 m wide. Contamination has been detected at depths greater than 100 m. The site is underlain by an unconfined aquifer. The surface topography can be approximated as a gentle slope, falling more than 13 m over a distance of 1.3 km. The release of volatile organic chemicals to the atmosphere from a coarse vadose zone can be significant. Locating the points of greatest vapor release was one of the objectives of the study. Thus, the top surface could not be modeled as a no-flow boundary. Boundary blocks representing the atmosphere were needed.

A 2,300-cell two-dimensional grid was developed that contained boundary blocks on the upgradient and downgradient sides, as well as large atmospheric blocks on the top boundary. The

bedrock and the alluvial soil were assumed to be uniform. The vadose zone grid blocks were assigned a thickness of 1 m. The length of the blocks was 20 m.

One key feature of the domain was the spatial variation in soil-bedrock contact. The porosity and permeability of the soil and bedrock were obtained from field measurements. Soil porosity was found to be a linear function of depth. Bedrock porosity was estimated from fracture spacing and permeability using the cubic law (Witherspoon and Gale, 1977; Witherspoon et al., 1980) and its refinements (Zimmerman et al., 1991; Zimmerman et al., 1992). Bedrock blocks were highly fractured; their permeability was not insignificant. Capillary pressure parameters were taken from laboratory measurements, modified to match field data, and used to obtain parameters for the functions of Parker et al. (1987). The relative permeability functions of Stone (1970) were used (IRP = 6).

Preliminary two-phase runs were conducted to reach steady state. These runs generated the initial conditions for subsequent runs. The first run concerned only the unsaturated blocks of the upgradient boundary. Above the column was a semi-infinite atmospheric boundary block, and below the column was a semi-infinite water table block (Figure 1a). The atmospheric block had a "rock grain specific heat" set 1,000 times higher than the soil formation, a permeability of 10^{-5} m^2, and a porosity of 1.0. The relative permeability of the block to air would be 1.0, and the permeability to water would be nearly zero. Thus, IRP was set to 2 and RP(1) was set to 20. The capillary pressure functions for the atmosphere were the "zero capillary pressure" functions, i.e., ICP = 9. The water table block had properties similar to the alluvial soil, except that the relative permeability was 1.0 in all phases (IRP = 5, "all perfectly mobile") and the zero capillary pressure functions were used (ICP = 9). Temperature, atmospheric pressure, and humidity data were obtained from government sources (Quayle and Presnell, 1991) and corrected as necessary. Pressure, for example, was corrected for elevation to the nearest pascal. Initial conditions for the capillary pressure in the vadose zone were precalculated using the model of van Genuchten (1980). Steady state was attained from the twentieth time step.

The determination of the pressure in the saturated portion of the upgradient boundary was computed separately, using the water table block described above as the upper boundary condition. The air pressure for the top boundary blocks was obtained by means of a horizontal one-dimensional run for the atmospheric blocks (Figure 1b). The boundary conditions were imposed on the system by the upgradient boundary block. The slope was simulated by means of the cosine parameter BETAX in the connections inputs. The initial pressures for the downgradient boundary were obtained in two steps following the method used for the upgradient side, using the properties of the most downgradient block of the horizontal run as a boundary condition.

With the boundary conditions established, it was possible to compute the steady-state pressures and saturations for the interior of the domain (Figure 2). Connecting semi-infinite atmospheric boundary blocks to the domain will result in desiccation unless recharge rates are provided for the surface blocks. There were four zones based on land use. The initial conditions for interior cells were determined from the van Genuchten (1980) model and the hydrostatic equation, based on the location of the water table and the bedrock-alluvium contact. About 500 time steps were needed to reach steady state. The steady-state run helped establish the location of the water table in the expanses between available data.

The T2VOC model was then run for three phases with a TCE source at the location of the release. Warm start simulations were then conducted for the period following the termination of the release. The properties of TCE were obtained from Reid et al. (1987).

Results

The model output gives a history of the flow. Figure 3 shows the TCE concentrations after 16 years. In the simulation, the dissolved-phase contamination arrived ahead of any DNAPL. TCE

vapor emanated from the water table. TCE vapor concentrations were highest just above the water table; this should be expected. Where density-driven flow is the dominant soil-vapor transport mechanism, dense TCE vapor will move along the water table. Where vapors move by a combination of dissolved-phase transport and Henry's Law partitioning, TCE concentrations will be highest near their source, the groundwater. Density-driven flow was favored nearer to the source of the release, and dissolved-phase transport further from the source.

The concentrations of TCE at the water table do not drop steadily as a function of horizontal distance from the source. In any given vertical cross section, there is a depth at which the maximum TCE groundwater concentration occurs. This maximum groundwater TCE concentration is progressively deeper as one moves downgradient. The TCE concentration at the water table is affected by the distance between the water table and the level of maximum concentration.

In the neighborhood of the source, the output shows how the DNAPL sinks to the less conductive bedrock. Although DNAPL penetrated the bedrock in places, a DNAPL pool formed at a local low in the soil-bedrock surface. The concentration of TCE gas was greatest just above the water table. An examination of TCE vapor concentrations along air-soil surface blocks shows that the highest concentrations were associated with the bedrock high, and the location directly above the point of the release. There was also a local maximum just upgradient of a high recharge zone.

One input parameter that has not been discussed so far is the width of the two-dimensional grid blocks. Clearly, concentrations are strongly affected by the volume of the formation into which it is assumed the contamination was released. In the above simulation, it was assumed that the blocks were 1 m wide. Since there is no force or structure corralling the contamination into a 1-m-wide corridor, this simulation can be taken to be a high transport end member. The simulation was repeated using a domain width of 300 m. This width is the approximate width of the 1,000 mg/m^3 contour. The significance of 1,000 mg/m^3 is that this is the concentration at the downgradient end of the domain. Figure 4 shows the modeled concentration of TCE in the groundwater after 16 years.

Discussion

The results of the second simulation were in better agreement with field data. However, near the source, this simulation failed to predict the DNAPL that has been found at depth. When very wide blocks are used in a two-dimensional simulation, the organic contaminant mass can be spread out to a point that it is difficult to attain concentrations in excess of the solubility necessary to produce the DNAPL that has been observed beneath the source. The proportion of TCE mass entering into the atmospheric blocks above the source is also increased by having wide blocks. The thermodynamic equations in T2VOC interpret the spreading out of the contaminant mass of a chemical such as TCE in terms of enhanced volatilization. Thus, widening the blocks yielded a mixed result in terms of the accuracy of the simulation: gains in accuracy downgradient from the source were achieved at a cost in accuracy closer to the source. The volume of DNAPL was underpredicted, and the rate of volatilization was overpredicted.

Conclusion

T2VOC model output is useful in simulating the transport of volatile chemicals in a realistic subsurface environment that includes the unsaturated zone. This is particularly true if the release occurred in the unsaturated zone, and when it is of interest to predict the release of soil gas into buildings. The contribution of soil-vapor transport to the spread of groundwater contamination was manifested by the arrival of detectable levels of TCE at the downgradient side of the domain seven years ahead of the time one would predict from its retarded velocity. However, density-driven flow was not exhibited in these simulations in every part of the domain with the chosen gridding scheme.

Two-dimensional simulations can overestimate the transport of the contaminant at great distance from the source if the domain thickness is too small. They can omit a free-phase liquid near the source and overestimate vapor flux near the source if the thickness is too great. Three-dimensional modeling avoids this difficulty. However, within the constraints many environmental problems must be solved, three-dimensional modeling can be inconvenient and its cost is prohibitive to many industrial clients. Thus, when T2VOC is used in a real-life industrial setting, careful choices must be made in determining the grid.

References

Falta, R. W., K. Pruess, S. Finsterle, and A. Battistelli, 1994, T2VOC User's Guide, Lawrence Berkeley Laboratory, Berkeley, CA, (LBL report number pending).

Moridis, G. J. and K. Pruess, 1995, T2CG1: A Package of Preconditioned Conjugate Gradient Solvers for the TOUGH2 Family of Codes, LBL Report Number 36235, Lawrence Berkeley Laboratory, Berkeley, CA.

Parker, J. C., R. J. Lenhard, and T. Kuppusamy, 1987, A Parametric Model for Constitutive Properties Governing Multiphase Flow in Porous Media, *Water Res. Res., 23*, (4), 618-624.

Quayle, R. and W. Presnell, 1991, Climatic Averages and Extremes for U.S. Cities, Historical Climatology Series 6-3, U.S. Department of Commerce, National Oceanic and Atmospheric Administration, Asheville, NC.

Reid, R. C., J. M. Prausnitz, and B. E. Poling, 1987, *The Properties of Gases and Liquids,* McGraw-Hill, New York.

Rivett, M. O., 1995, Soil-Gas Signatures from Volatile Chlorinated Solvents: Borden Field Experiments, *Ground Water 33*, (1), 84-98.

Stone, H. L., 1970, Probability Model for Estimating Three-Phase Relative Permeability, *J. Pet. Tech., 22*, (1), 214-218.

van Genuchten, M. Th., 1980, A Closed-Form Equation for Predicting the Hydraulic Conductivity of Unsaturated Soils, *Soil Sci. Soc. Am. J., 44*, 892-898.

Witherspoon, P. A. and J. E. Gale, 1977, Mechanical and Hydraulic Properties of Rocks Related to Induced Seismicity, *Eng. Geol. 11*, 23-57.

Witherspoon, P. A., J. S. Y. Wang, K. Iwai, and J. E. Gale, 1980, Validity of Cubic Law for Fluid Flow in a Deformable Rock Fracture, *Water Res. Res., 16*, (6), 1016-1024.

Zimmerman, R. W., S. Kumar, and G. S. Bodvarsson, 1991, Lubrication Theory Analysis of the Permeability of Rough-walled Fractures, *Int. J. Rock Mech. Min. Sci. & Geomech. Abstr. 28*, (4), 325-331.

Zimmerman, R. W., D.-W. Chen, and N. G. W. Cook, 1992, The Effect of Contact Area on the Permeability of Fractures, *J. Hydrol., 139*, 79-96.

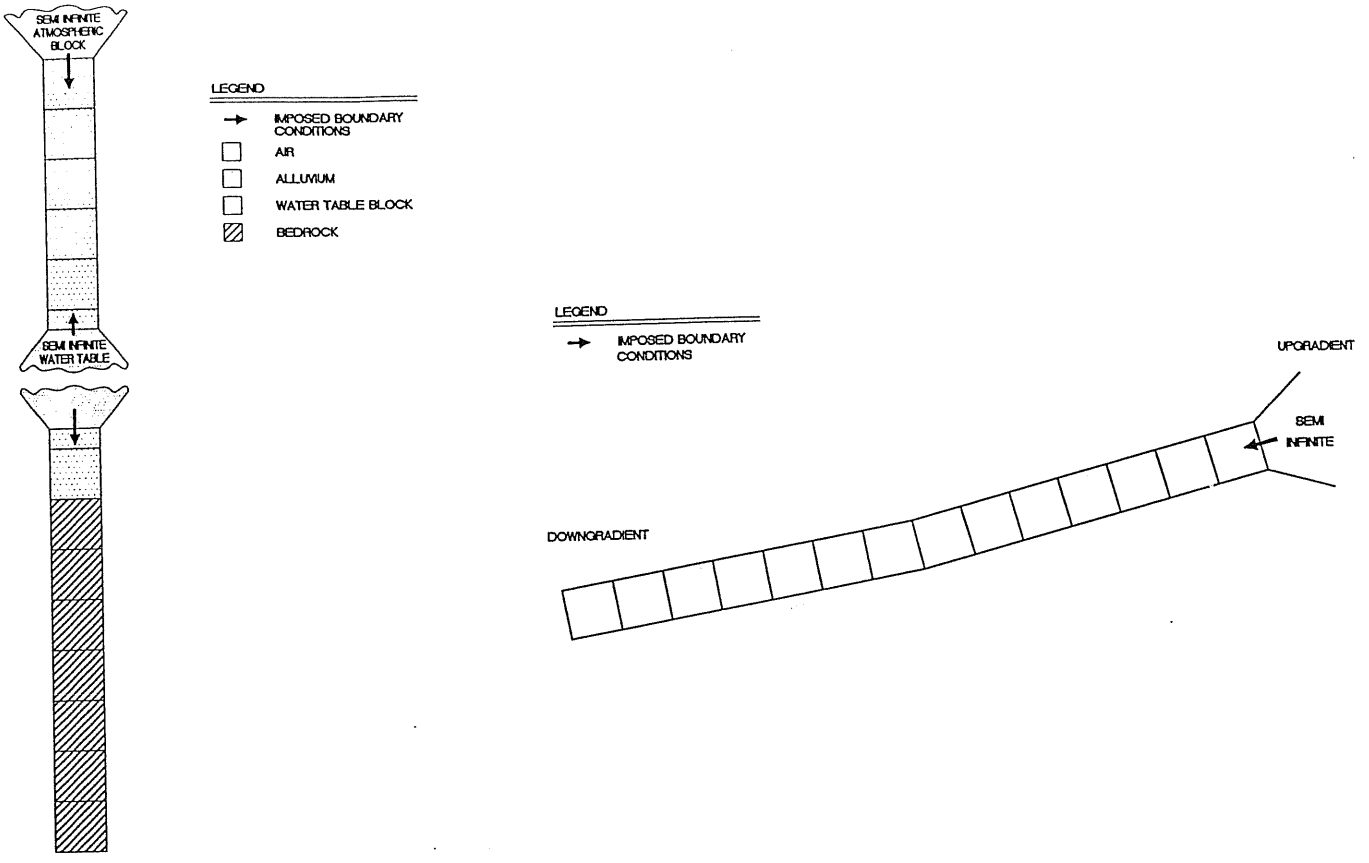

Figure 1. (a) Schematic representation of the upgradient boundary block calibration.
(b) Schematic representation of the atmospheric boundary block calibration.

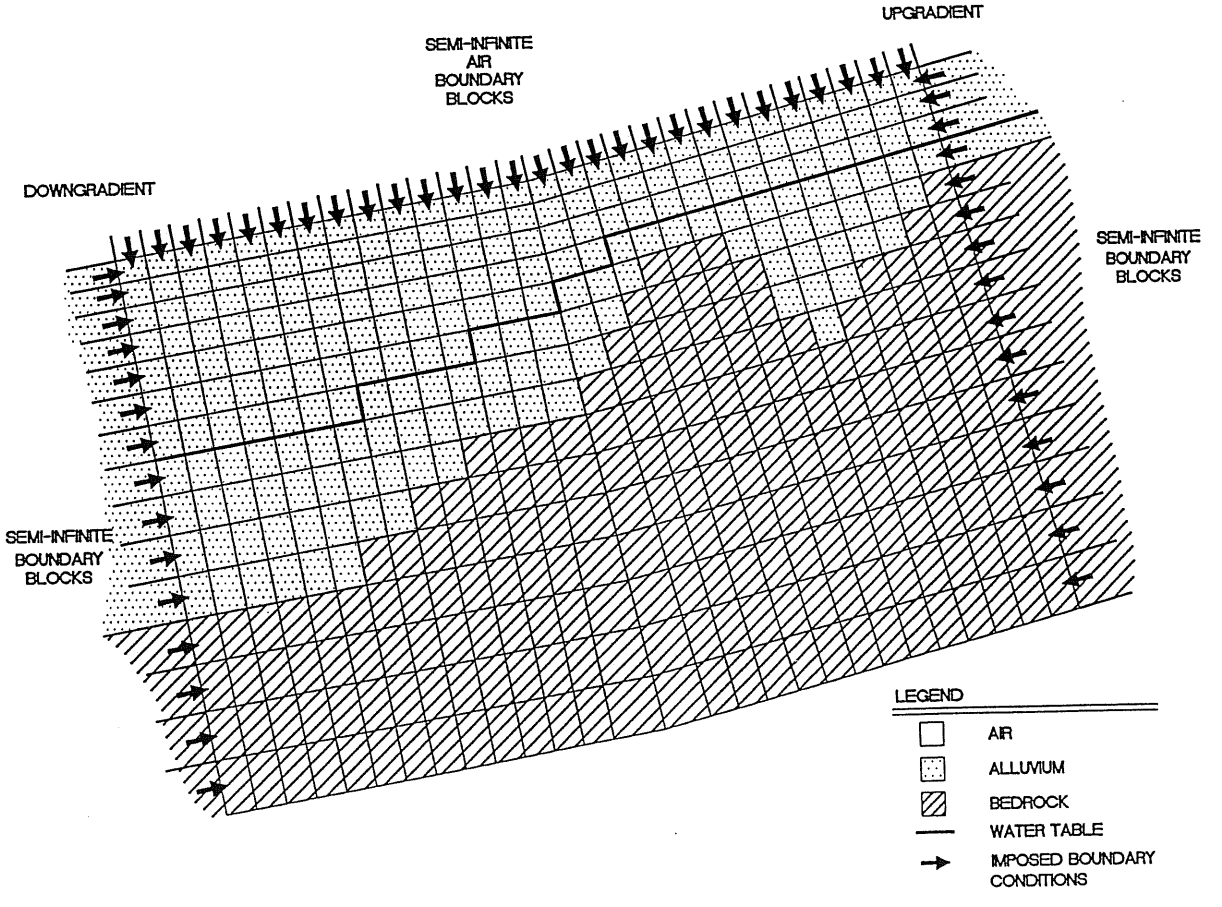

Figure 2. Schematic representation of the two-dimensional domain.

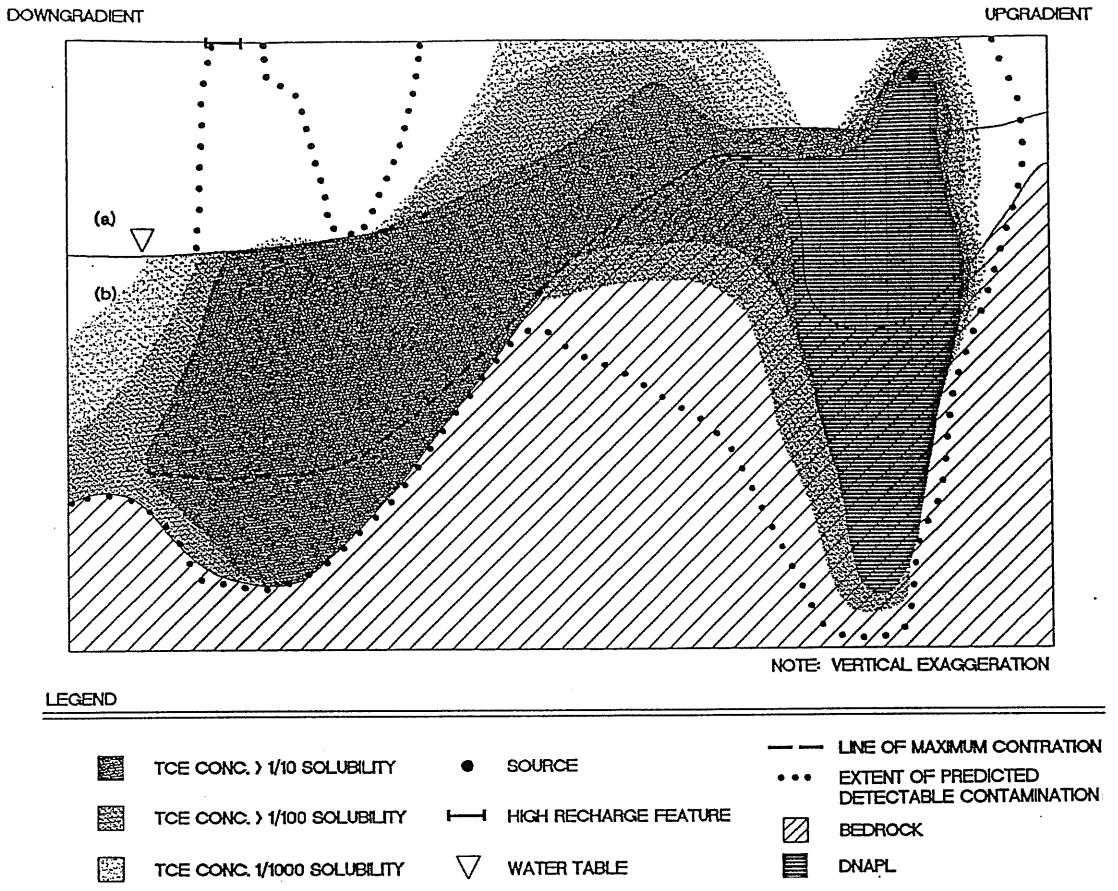

Figure 3. TCE concentrations after 16 years for the 1-m wide domain: (a) soil vapor in the vadose zone, (b) dissolved phase contamination in the groundwater.

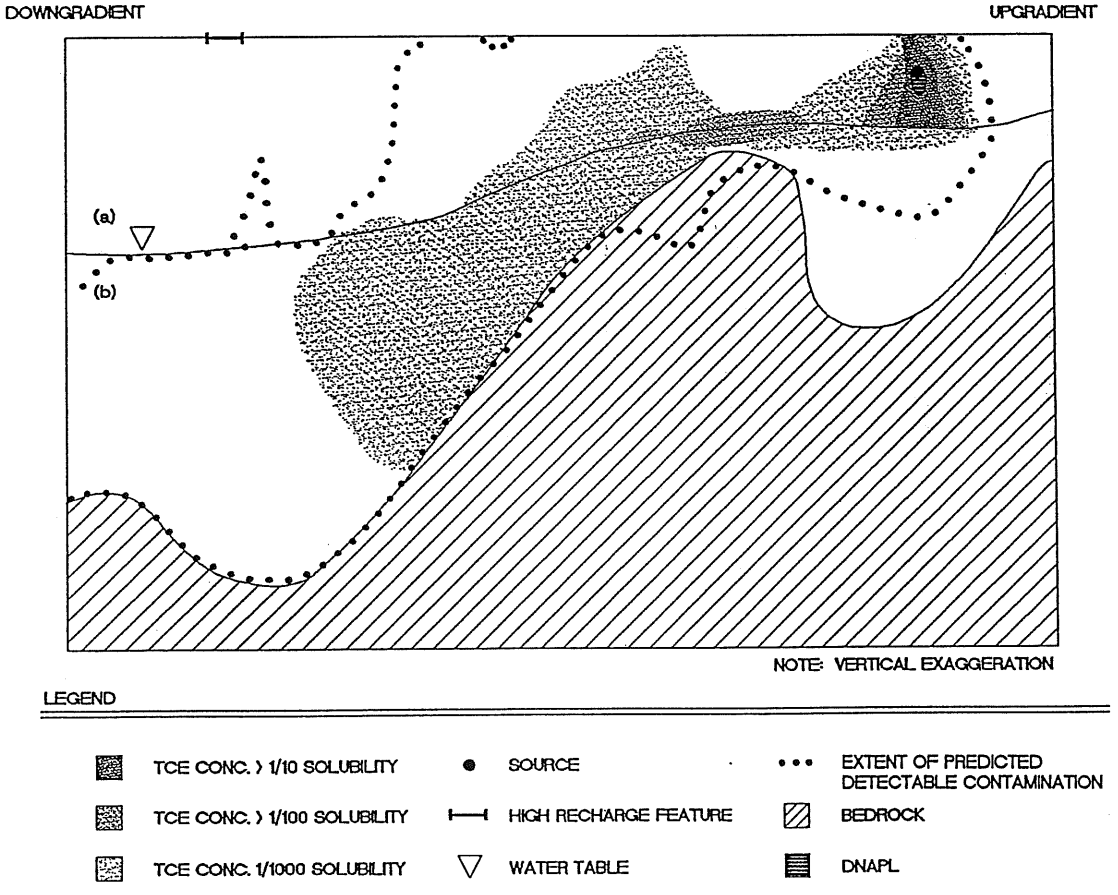

Figure 4. TCE concentrations after 16 years for the 300-m wide domain: (a) soil vapor in the